J|A|C|S ARTICLES

Published on Web 10/13/2009

Roles of Surface Steps on Pt Nanoparticles in Electro-oxidation of Carbon Monoxide and Methanol

Seung Woo Lee,[†,⊥] Shuo Chen,[‡,⊥] Wenchao Sheng,[§,⊥] Naoaki Yabuuchi,[‡,⊥] Yong-Tae Kim,[‡,⊥,#,&] Tadaoki Mitani,[#] Elio Vescovo,[▽] and Yang Shao-Horn*[,‡,∥,⊥]

Department of Chemical Engineering, Department of Mechanical Engineering, Department of Chemistry, Department of Materials Science and Engineering, and Electrochemical Energy Laboratory, Massachusetts Institute of Technology, Cambridge, Massachusetts 02139, School of Materials Science, Japan Advanced Institute of Science and Technology, Ishikawa 923-1292, Japan, and Brookhaven National Laboratory, Upton, New York 11973-5000

Received March 31, 2009; E-mail: shaohorn@mit.edu

Abstract: Design of highly active nanoscale catalysts for electro-oxidation of small organic molecules is of great importance to the development of efficient fuel cells. Increasing steps on single-crystal Pt surfaces is shown to enhance the activity of CO and methanol electro-oxidation up to several orders of magnitude. However, little is known about the surface atomic structure of nanoparticles with sizes of practical relevance, which limits the application of fundamental understanding in the reaction mechanisms established on single-crystal surfaces to the development of active, nanoscale catalysts. In this study, we reveal the surface atomic structure of Pt nanoparticles supported on multiwall carbon nanotubes, from which the amount of high-index surface facets on Pt nanoparticles is quantified. Correlating the surface steps on Pt nanoparticles with the electrochemical activity and stability clearly shows the significant role of surface steps in enhancing intrinsic activity for CO and methanol electro-oxidation. Here, we show that increasing surface steps on Pt nanoparticles of ∼2 nm can lead to enhanced intrinsic activity up to ∼200% (current normalized to Pt surface area) for electro-oxidation of methanol.

Introduction

Studies on well-defined model systems such as single-crystal surfaces have led to the determination of surface reaction mechanisms and identification of physical parameters such as electronic structure[1] and surface atomic structure[2] that govern activity. In particular, increasing steps and kinks on single-crystal Pt surfaces has been shown to enhance the activity of electro-oxidation of carbon monoxide (CO) and methanol.[3−6] CO electro-oxidation can be catalyzed by preferential adsorption of oxygenated species on the under-coordinated sites,[3] while methanol electro-oxidation can be assisted similarly by adsorbed oxygenated species in the indirect pathway, and via direct methanol oxidation[4] and methanol decomposition[7] at the step sites in the direct pathway. Extending electrochemical oxidation reaction mechanisms established on model single-crystal surfaces to design of active nanoscale catalysts[8] is not straightforward. Although high-index surfaces [(100) steps on (100) terraces] were shown to increase the activity of formic acid and ethanol oxidation on Pt nanoparticles of ∼50 nm and larger,[9] there is no previous experimental evidence to conclusively show the role of surface steps on Pt nanoparticles with sizes of practical relevance (typically ∼5 nm) on the electro-oxidation activity of CO and methanol.

One of the intensively debated issues over the last two decades is centered on whether and how nanoparticle activity for CO and methanol electro-oxidation should be size dependent. However, both nanoparticle size and nanoparticle surface atomic structure can influence activity. Particle size reduction increases the density of surface under-coordinated sites as decreasing crystal size of a given particle shape such as truncated octahedron[10] increases the fractions of surface atoms on the

[†] Department of Chemical Engineering, Massachusetts Institute of Technology.
[‡] Department of Mechanical Engineering, Massachusetts Institute of Technology.
[§] Department of Chemistry, Massachusetts Institute of Technology.
[∥] Department of Materials Science and Engineering, Massachusetts Institute of Technology.
[⊥] Electrochemical Energy Laboratory, Massachusetts Institute of Technology.
[#] Japan Advanced Institute of Science and Technology.
[▽] Brookhaven National Laboratory.
[&] Present address: School of Mechanical Engineering, Pusan National University, Pusan 609-735, Korea.

(1) Stamenkovic, V. R.; Fowler, B.; Mun, B. S.; Wang, G. F.; Ross, P. N.; Lucas, C. A.; Markovic, N. M. *Science* **2007**, *315*, 493–497.
(2) Jaramillo, T. F.; Jorgensen, K. P.; Bonde, J.; Nielsen, J. H.; Horch, S.; Chorkendorff, I. *Science* **2007**, *317*, 100–102.
(3) Lebedeva, N. P.; Koper, M. T. M.; Feliu, J. M.; van Santen, R. A. *J. Phys. Chem. B* **2002**, *106*, 12938–12947.
(4) Housmans, T. H. M.; Koper, M. T. M. *J. Phys. Chem. B* **2003**, *107*, 8557–8567.
(5) Adzic, R. In *Modern Aspects of Electrochemistry*; Bockris, J. O. M., Conway, B. E., White, R. E., Eds.; Springer: New York, 1990; Vol. 21, pp 163−236.
(6) Lai, S. C. S.; Lebedeva, N. P.; Housmans, T. H. M.; Koper, M. T. M. *Top. Catal.* **2007**, *46*, 320–333.
(7) Shin, J. W.; Korzeniewski, C. *J. Phys. Chem.* **1995**, *99*, 3419–3422.
(8) *Catalysis and Electrocatalysis at Nanoparticle Surfaces*; Wieckowski, A., Savinowa, E., Vayenas, C. G., Eds.; Marcel Dekker, Inc.: New York, 2003.
(9) Tian, N.; Zhou, Z. Y.; Sun, S. G.; Ding, Y.; Wang, Z. L. *Science* **2007**, *316*, 732–735.

corner and edge sites.[11] However, decreasing particle sizes does not always lead to higher intrinsic activity for nanoparticles as one would expect, to a first approximation, based on stepped single-crystal Pt studies,[6] where the underlying mechanism for this phenomenon is not understood. A number of studies have shown lower activity for adsorbed CO or methanol electro-oxidation on smaller Pt nanoparticles,[12−18] while others report an opposite trend.[8,11,19] This discrepancy may be attributed to the hypothesis that the surface structures of nanoparticles in these previous studies, which are typically not characterized, may change with different sizes and influence activity to a greater extent than particle size reduction. This work aims to bridge the gap in the fundamental understanding of the electro-oxidation activity for CO and methanol between nanoparticles and single-crystal surfaces by revealing the surface and electronic structures of Pt nanoparticles using high-resolution transmission electron microscopy (HRTEM) and ultraviolet photoelectron spectroscopy (UPS). In this study, the surface characteristics of Pt nanoparticles of very comparable sizes are correlated with the intrinsic activity for CO and methanol electro-oxidation. Here, we show that high-index surfaces, particularly steps on the (111) surfaces, can play a very important role in enhancing intrinsic activity for CO and methanol electrochemical oxidation on Pt nanoparticles of ~2 nm.

Results and Discussion

Surface Atomic Structure Characteristics of Pt Nanoparticles. Pt nanoparticles supported on multiwall carbon nanotubes (MWNTs) were prepared by the single atom to cluster (SAC) approach,[20] which included (1) reduction of $H_2[PtCl_6]$ with $NaBH_4$ on thiolated MWNTs and (2) elimination of the thiol groups by a heat-treatment in H_2 to form Pt nanoparticles (the fraction of Pt in Pt/MWNTs is 20 wt %) in the range from 548 to 773 K. Pt nanoparticles obtained from different temperatures were found dispersed uniformly on MWNTs (Figures 1a and S1). The number-averaged (d_n) particle diameters of Pt nanoparticles obtained from different heat-treatment temperatures in the range from 548 to 773 K were found very similar, ~2 nm, as shown in Figure 1b. Combination of HRTEM images and their fast Fourier transforms (FFTs) allowed the identification of surface facets of Pt nanoparticles and showed that Pt nanoparticles obtained at lower temperatures exhibited higher fractions of high-index surface facets. Representative HRTEM images and FFTs of Pt particles in the Pt/MWNT samples heat-treated at 573 and 673 K are shown in Figure 1c and d, respectively, where surface atomic structures are revealed clearly. Not only were low-index surfaces found but also high-index surfaces in the groups of n(111) × (111), n(111) × (100), and n(100) × (111) were noted (Figure 1c−e).

The length fractions of low-index and high-index planes along the particle perimeter projected along the [110] zone axis of individual Pt nanoparticles could be measured from HRTEM images (Figure S2). Provided that Pt nanoparticles have shapes that are close to a truncated octahedron,[10,21,22] the surface area fractions of low-index and high-index facets are comparable to their corresponding length fractions (Figure S3). The area fractions of all observed high-index surface facets of Pt nanoparticles were found to decrease with increasing heat-treatment temperature, as shown in Figure 1f. This trend was particularly notable for stepped surfaces on the (111) terrace, where the (111) and (100) steps were found to decrease considerably with increasing heat-treatment temperature (Figure S2f). The observed changes in the surface atomic structure of Pt nanoparticles may be explained by considering the formation mechanism of Pt nanoparticles via the single atom to cluster (SAC) approach.[20] It is hypothesized that Pt atoms do not have sufficient mobility nor time to fully reach the thermodynamically stable shape, truncated octahedron[10,23] with only low-index surfaces of (111) and (100), at lower heat-treatment temperatures, while increasing mobility of Pt atoms at higher heat-temperatures can reduce and replace high-index surfaces with higher surface energy by low-index planes with lower surface energy.[24,25] Remarkably, we note that the area fraction of high-index planes on Pt nanoparticles can change up to 50% even though there is less than ~1 nm of difference in the number-averaged (d_n) particle diameters of Pt/MWNT samples obtained in the temperature range from 548 to 773 K in Figure 1f.

Surface Electronic Structure Characteristics of Pt Nanoparticles. We then examined the effect of surface atomic structure on the surface electronic structure of Pt/MWNT samples after exposure to ambient atmosphere with UPS. Increasing surface steps found on Pt nanoparticles in the Pt/MWNT samples obtained at lower temperatures lowers the coordination number of surface atoms, which can greatly influence the adsorption of oxygenated species and thus the activity for CO and methanol electro-oxidation. First-principle studies have shown that under-coordinated atoms on the steps and kinks of high-index surfaces have narrowed surface d band and upshifted d band center relative to the Fermi level,[26] which can result in stronger binding of O[27,28] on these under-coordinated sites. Figure 2a shows the partial valence band structure of the Pt/MWNT samples and a MWNT sample. The sole photoemission contribution from Pt nanoparticles was obtained by subtracting the density of states of MWNT from those of Pt/MWNT samples,[29] which is shown in the inset of Figure 2b. With increasing heat-treatment

(10) Frenken, J. W. M.; Stoltze, P. *Phys. Rev. Lett.* **1999**, *82*, 3500–3503.
(11) Kinoshita, K. *J. Electrochem. Soc.* **1990**, *137*, 845–848.
(12) Park, S.; Xie, Y.; Weaver, M. J. *Langmuir* **2002**, *18*, 5792–5798.
(13) Maillard, F.; Savinova, E. R.; Stimming, U. *J. Electroanal. Chem.* **2007**, *599*, 221–232.
(14) Maillard, F.; Eikerling, M.; Cherstiouk, O. V.; Schreier, S.; Savinova, E.; Stimming, U. *Faraday Discuss.* **2004**, *125*, 357–377.
(15) Mayrhofer, K. J. J.; Arenz, M.; Blizanac, B. B.; Stamenkovic, V.; Ross, P. N.; Markovic, N. M. *Electrochim. Acta* **2005**, *50*, 5144–5154.
(16) Frelink, T.; Visscher, W.; Vanveen, J. A. R. *J. Electroanal. Chem.* **1995**, *382*, 65–72.
(17) Mayrhofer, K. J. J.; Blizanac, B. B.; Arenz, M.; Stamenkovic, V. R.; Ross, P. N.; Markovic, N. M. *J. Phys. Chem. B* **2005**, *109*, 14433–14440.
(18) Arenz, M.; Mayrhofer, K. J. J.; Stamenkovic, V.; Blizanac, B. B.; Tomoyuki, T.; Ross, P. N.; Markovic, N. M. *J. Am. Chem. Soc.* **2005**, *127*, 6819–6829.
(19) Chen, L.; Lu, G. X. *Electrochim. Acta* **2008**, *53*, 4316–4323.
(20) Kim, Y. T.; Ohshima, K.; Higashimine, K.; Uruga, T.; Takata, M.; Suematsu, H.; Mitani, T. *Angew. Chem., Int. Ed.* **2006**, *45*, 407–411.
(21) Stamenkovic, V. R.; Mun, B. S.; Arenz, M.; Mayrhofer, K. J. J.; Lucas, C. A.; Wang, G. F.; Ross, P. N.; Markovic, N. M. *Nat. Mater.* **2007**, *6*, 241–247.
(22) Gontard, L. C.; Chang, L.-Y.; Hetherington, C. J. D.; Kirkland, A. I.; Ozkaya, D.; Dunin-Borkowski, R. E. *Angew. Chem., Int. Ed.* **2007**, *46*, 3683–3685.
(23) Ferreira, P. J.; Shao-Horn, Y. *Electrochem. Solid-State Lett.* **2007**, *10*, B60–B63.
(24) Foiles, S. M.; Baskes, M. I.; Daw, M. S. *Phys. Rev. B* **1986**, *33*, 7983–7991.
(25) Skriver, H. L.; Rosengaard, N. M. *Phys. Rev. B* **1992**, *46*, 7157–7168.
(26) Hammer, B.; Nielsen, O. H.; Norskov, J. K. *Catal. Lett.* **1997**, *46*, 31–35.
(27) Gland, J. L.; Korchak, V. N. *Surf. Sci.* **1978**, *75*, 733–750.
(28) Han, B. C.; Miranda, C. R.; Ceder, G. *Phys. Rev. B* **2008**, *77*, 075410.

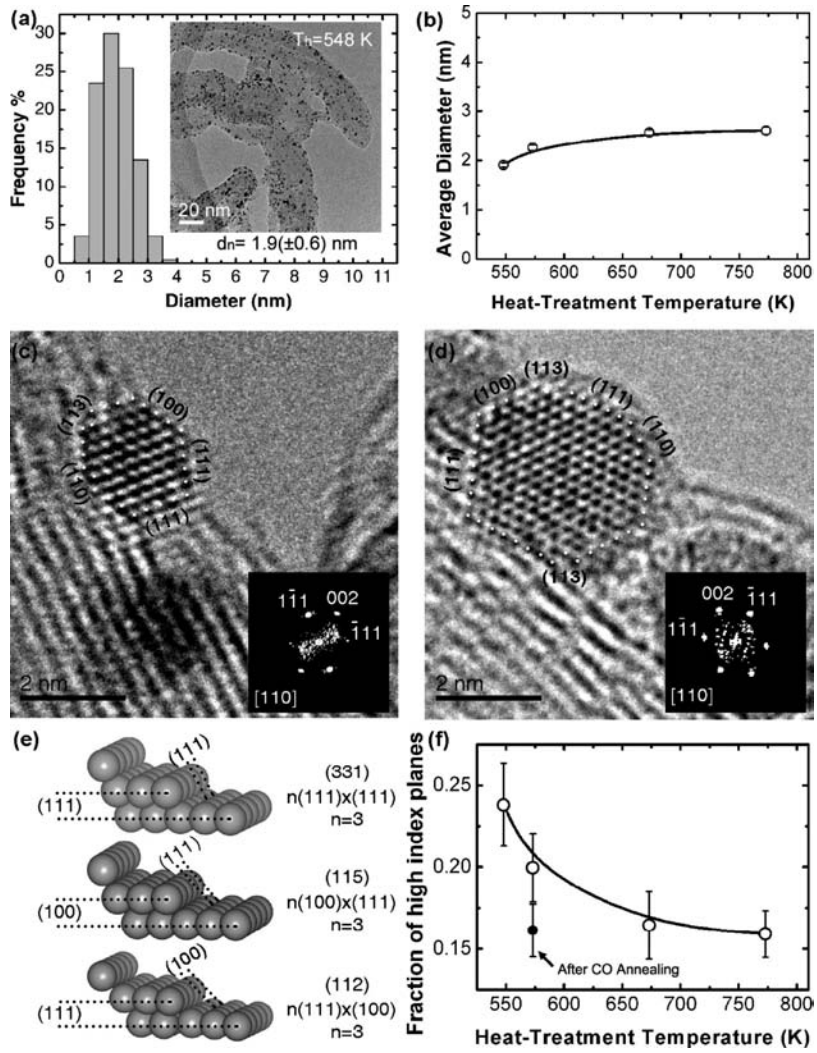

Figure 1. Particle sizes and surface atomic structure of Pt nanoparticles in the Pt/MWNT samples. (a) Histogram and typical TEM micrograph (inset) of a Pt/MWNT sample heat-treated at 548 K. (b) Number-averaged diameter (d_n) of Pt/MWNTs as a function of heat-treatment temperature. Standard deviation in d_n is ~1 nm, and error bars in the graph are based on standard deviation of the mean by considering >200 Pt nanoparticles per sample. (c,d) Typical HRTEM images and FFT results (inset) of Pt nanoparticles obtained from 573 and 673 K, respectively. (e) Schematics of high-index planes observed on Pt nanoparticles. (f) Average area fractions of all high-index planes observed in the Pt/MWNT samples as a function of heat-treatment temperatures. The solid circle corresponds to the 573 K sample that was cycled from 0.05 to 1.1 V vs RHE in CO-saturated 0.1 M $HClO_4$ solution (CO annealing). The calculation of error bars can be found in the Experimental Section.

temperatures, the density of states of Pt/MWNT in the range of −6 to −4 eV decreases, and the occupied states become narrowed and shifted up toward the Fermi level (E_F). As the photoemission cross-section of Pt is dominated by the d states at 80 eV because the photoemission cross-section of s and p states is much smaller than that of the d states, the valence band structure measured mostly reflects the valence d states.[30] The d band center relative to E_F, which was calculated using a method reported previously,[31] becomes less negative with increasing heat-treatment temperature, as shown in Figure 2b. This trend cannot be explained by the observed reduction of Pt surface coordination with decreasing heat-treatment temperature because this should lead to a narrowed surface d band and upshifted d band center relative to E_F.[26] On the other hand, increasing the number of oxygen neighbors has shown to cause d band broadening of surface atoms of Pt and Rh.[32,33] Therefore, observed d band broadening and lowering of the d band center of Pt/MWNT samples obtained from lower heat-treatment temperatures can be explained by the hypothesis that these Pt nanoparticles, with higher fractions of high-index surface facets, have higher surface oxygen coverage than those prepared at higher temperatures upon exposure to ambient atmosphere. It should be noted that the oxygen surface coverage on Pt nanoparticles of 548 K is still very small as the UPS Pt 4f core level, which is less surface sensitive than valence spectra, showed no significant shift relative to bulk Pt[34] (Figure S4). Similarly, no significant change was found in the coordination number of the nearest neighbor Pt−Pt and Pt−O (Figure S5a

(29) Eberhardt, W.; Fayet, P.; Cox, D. M.; Fu, Z.; Kaldor, A.; Sherwood, R.; Sondericker, D. *Phys. Rev. Lett.* **1990**, *64*, 780–784.
(30) Yeh, J. J.; Lindau, I. *At. Data Nucl. Data Tables* **1985**, *32*, 1–155.
(31) Mun, B. S.; Watanabe, M.; Rossi, M.; Stamenkovic, V.; Markovic, N. M.; Ross, P. N. *J. Chem. Phys.* **2005**, *123*, 204717.
(32) Lynch, M.; Hu, P. *Surf. Sci.* **2000**, *458*, 1–14.
(33) Ganduglia-Pirovano, M. V.; Scheffler, M.; Baraldi, A.; Lizzit, S.; Comelli, G.; Paolucci, G.; Rosei, R. *Phys. Rev. B* **2001**, *6320*, 205415.
(34) Legare, P.; Lindauer, G.; Hilaire, L.; Maire, G.; Ehrhardt, J. J.; Jupille, J.; Cassuto, A.; Guillot, C.; Lecante, J. *Surf. Sci.* **1988**, *198*, 69–78.

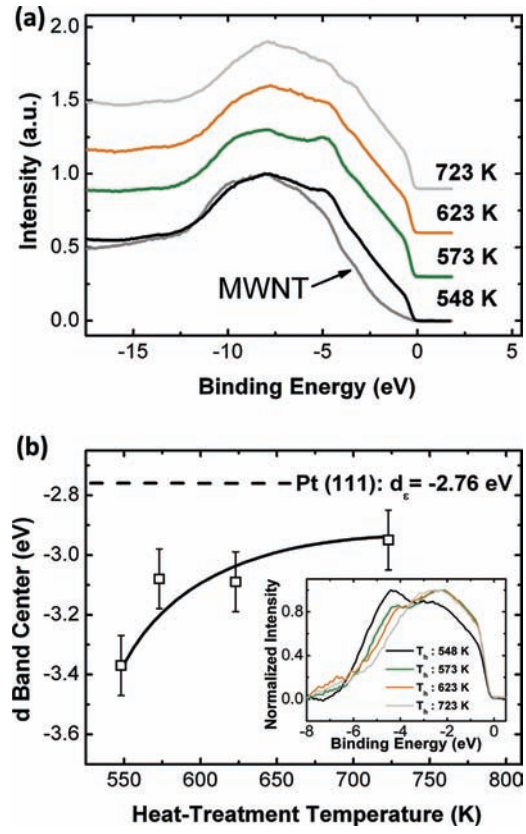

Figure 2. Partial valence band spectra of Pt/MWNT samples and Pt nanoparticles. (a) Outer-level photoemission spectra of Pt/MWNT samples obtained at different heat-treatment temperatures and a MWNT sample, which was collected at a photon energy of 80 eV. (b) Estimated d band center of occupied states (with largely Pt 5d character) of Pt nanoparticles[31] relative to that of single-crystal Pt (111).[1] The sole contribution from Pt was obtained by subtracting the photoemission of MWNT from those of the Pt/MWNT samples, and the spectra are shown in the inset of (b).

and b) and the Pt d band vacancy[35,36] (Figure S5c) from synchrotron X-ray adsorption data as a function of heat-treatment temperature because the technique provides signals averaged among surface and core atoms of Pt nanoparticles. While we cannot provide direct proof of increasing oxygenated species on Pt nanoparticles (having higher fractions of surface steps in Figures 1f and S2) obtained from decreasing heat-treatment temperature, UPS valence spectra can be rationalized by this hypothesis.

Intrinsic Activity of Pt Nanoparticles for CO Electro-oxidation. We first analyzed the electro-oxidation activity of CO on Pt/MWNT samples as CO commonly serves a model system to understand the electrocatalysis of small organic molecules[6,18,37,38] such as methanol. The intrinsic electro-oxidation activity of adsorbed CO (CO_{ad}) on Pt/MWNT samples was found to increase with decreasing heat-treatment temperature. Figures 3a and S6 show specific activity, defined as current normalized to electrochemical surface area (ESA) of Pt, as a function of potential versus reversible hydrogen electrode

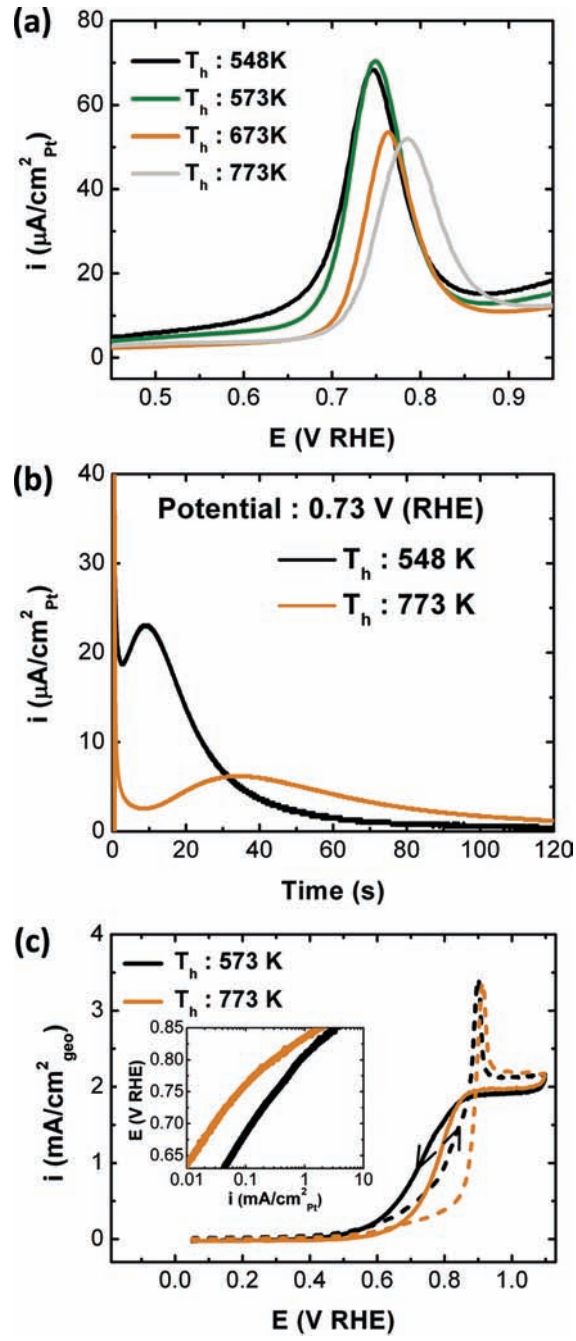

Figure 3. CO electro-oxidation activity on Pt/MWNT samples measured at room temperature. (a) Specific oxidation current (normalized to Pt ESA) of CO_{ad} on Pt/MWNT samples in 0.1 M $HClO_4$ with 5 mV/s. (b) Specific current transients (normalized to Pt ESA) of the oxidation of CO_{ad} after the potential was stepped from 0.1 to 0.73 V vs RHE. (c) RDE current density (normalized to RDE geometric area) of CO bulk oxidation at 1600 rpm, where the specific activity (normalized to Pt ESA) calculated from current in the negative potential sweep with 5 mV/s is shown in the inset.

(RHE). The onset and peak oxidation potentials of CO_{ad} on the Pt/MWNT samples shift to lower potentials with decreasing heat-treatment temperature. Further experimental evidence of enhanced CO_{ad} electro-oxidation kinetics with decreasing heat-treatment temperature is provided by chronoamperometric measurements, where the characteristic time to reach the current maximum can be related to the reciprocal of the reaction rate constant. With increasing potentials, shorter time was required to reach the current maximum and to complete CO oxidation, which could be attributed to increasing adsorption of oxygenated

(35) Mansour, A. N.; Cook, J. W.; Sayers, D. E. *J. Phys. Chem.* **1984**, *88*, 2330–2334.
(36) Mukerjee, S.; Srinivasan, S.; Soriaga, M. P.; McBreen, J. *J. Phys. Chem.* **1995**, *99*, 4577–4589.
(37) Markovic, N. M.; Ross, P. N. *Surf. Sci. Rep.* **2002**, *45*, 121–229.
(38) Strmcnik, D. S.; Tripkovic, D. V.; van der Vliet, D.; Chang, K. C.; Komanicky, V.; You, H.; Karapetrov, G.; Greeley, J.; Stamenkovic, V. R.; Markovic, N. M. *J. Am. Chem. Soc.* **2008**, *130*, 15332–15339.

species at higher voltages similar to those reported previously[3,18] (Figure S7). More importantly, the characteristic time to reach current maximum at a given potential decreased considerably for Pt/MWNT samples with decreasing heat-treatment temperature, indicating faster oxidation kinetics. Specific current transients of Pt/MWNT samples obtained from 548 and 773 K at 0.73 V are compared in Figure 3b, where the time to reach the current maximum for the 773 K sample is ~4 times longer than that of the 548 K sample, and the 773 K sample showed 40% oxidation of CO_{ad} in comparison to 80% oxidation for the 548 K sample after 30 s.

The enhanced specific activity for electro-oxidation of CO_{ad} on Pt nanoparticles obtained from lower temperatures (Figure 3) can be attributed to increasing and preferential adsorption of oxygen species associated with water dissociation on higher fractions of high-index surface facets (Figures 1f and S2). Oxidation of CO_{ad} in acid is known to proceed by the Langmuir−Hinshelwood reaction mechanism,[39] where CO_{ad} reacts with adsorbed oxygenated species to form CO_2. Although Arenz et al.[18] suggest that surface defect sites can influence CO_{ad} electro-oxidation of Pt nanoparticles, this study, for the first time, reveals and quantifies for surface under-coordinated sites, namely, high-index surface facets such as the (111) steps on the (111) surfaces in Figures 1f and S2, which can be correlated with enhanced intrinsic activity of CO_{ad} oxidation on Pt nanoparticles. Our results are in good agreement with the findings reported for the electro-oxidation activity of CO_{ad} on single-crystal Pt stepped (111) surfaces, where the intrinsic activity is enhanced significantly with increasing (111) step density.[3] It should be pointed out that the proposed physical origin of activity enhancement of electro-oxidation of CO_{ad} in the Pt/MWNT samples is different from some previous studies of Pt nanoparticles,[13,14] where decreasing activity with smaller particle sizes has been attributed to reduced mobility of CO_{ad} as a result of stronger adsorption of CO on Pt sites with lower coordination.

Intrinsic activity of bulk CO electro-oxidation was also found to increase on Pt/MWNT samples with decreasing heat-treatment temperatures. Current was obtained from scanning a rotating disk electrode (RDE) in a CO-saturated solution as a function of potential (Figure S8). Geometric current densities (normalized to RDE area) of Pt/MWNT samples heat-treated at 573 and 773 K are compared in Figure 3c. Specific CO oxidation activity on the oxidized Pt surface in the negative-going scan, which is normalized to the Pt ESA, was found to increase with decreasing heat-treatment temperature, as shown in the inset of Figure 3c. At a potential of 0.7 V vs RHE, the specific current of the 573 K sample is 0.13 mA/cm^2_{Pt} as compared to 0.03 mA/cm^2_{Pt} for the 773 K sample, indicating higher activity for the samples heat-treated at lower temperatures. In addition, it is interesting to note that the Pt/MWNT sample obtained at 573 K with a d_n of ~2 nm exhibits much higher specific activity (1 mA/cm^2_{Pt} at 0.8 V vs RHE) than a CO-annealed, commercial Pt catalyst sample with a smaller diameter having d_n of ~1 nm (~0.05 mA/cm^2_{Pt} at 0.8 V vs RHE) reported previously.[17] This observation suggests that factors beyond particle size are important, and knowing the surface atomic structure and chemistry of nanoparticles is essential to understand, predict, and enhance the electro-oxidation activity of CO on Pt.

A very recent study of Pt single-crystal surfaces[38] has shown that even a modest number of potential cycling in CO-saturated solution (CO annealing[18]) can dramatically reduce surface adislands and decrease CO electro-oxidation activity. In addition, CO annealing has shown to decrease CO electro-oxidation activity of Pt nanoparticles.[18] However, correlation between such a structure change and CO electro-oxidation activity on Pt nanoparticles during CO annealing has not yet been investigated, despite significant technical importance. Pt/MWNT sample obtained at 573 K was cycled in a CO-saturated solution from 0.1 to 1.1 V vs RHE at a scan rate of 50 mV/s for 10 min (CO annealing). Intrinsic activity for electro-oxidation of CO_{ad} (CO stripping data in Figure 4a and chronoamperometric data in Figure 4b) and for bulk CO-electro-oxidation (Figure 4c) decreased considerably on Pt/MWNT sample obtained at 573 K after CO annealing. The number-averaged (d_n) particle diameters of Pt/MWNTs heat-treated at 573 K before and after CO annealing were found comparable, ~2.5 nm, as shown in

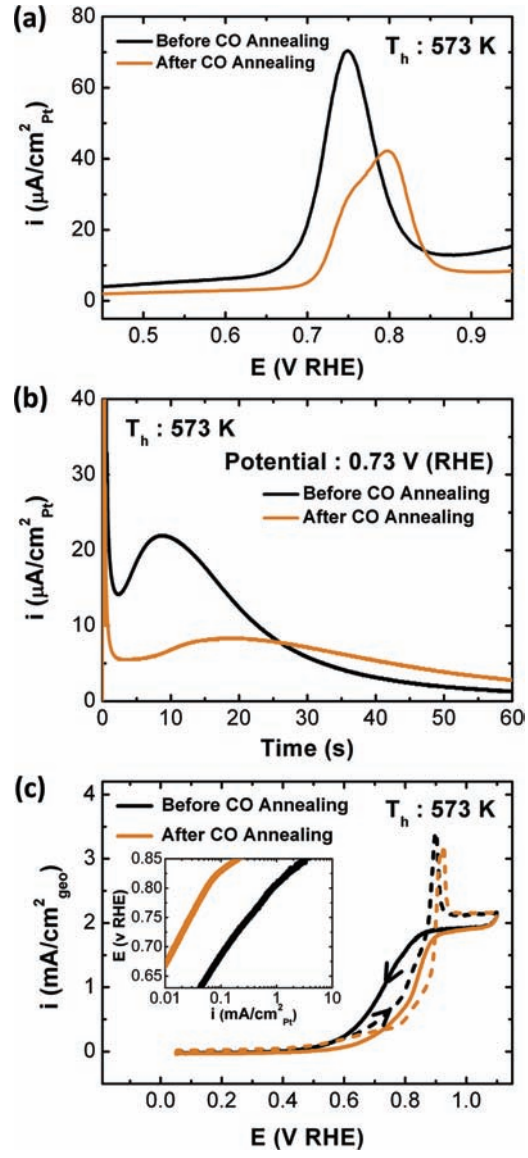

Figure 4. Comparison of CO electro-oxidation activity on Pt/MWNTs of 573 K before and after CO annealing. (a) Specific oxidation current (normalized to Pt ESA) of CO_{ad} on Pt/MWNT sample in 0.1 M $HClO_4$ with 5 mV/s. (b) Specific current transients (normalized to Pt ESA) of the oxidation of CO_{ad} after the potential was stepped from 0.1 to 0.73 V vs RHE. (c) RDE geometric current density of CO bulk oxidation at 1600 rpm, where the specific activity (normalized to Pt ESA) calculated from current in the negative potential sweep with 5 mV/s is shown in the inset.

(39) Gilman, S. *J. Phys. Chem.* **1964**, *68*, 70–80.

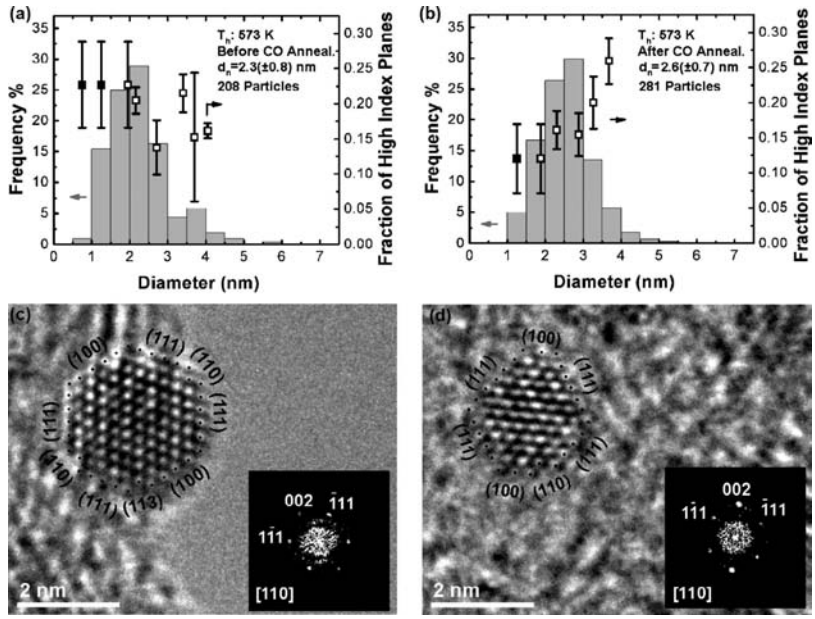

Figure 5. Pt particle size distribution (left axis) and area fraction of high-index planes (right axis) in Pt/MWNTs heat treated at 573 K before (a) and after (b) CO annealing, respectively. (c,d) Typical HRTEM image and FFT of a Pt nanoparticle in the Pt/MWNT sample after CO annealing. The calculation of error bars can be found in the Experimental Section.

Figure 5a and 5b. Two representative HRTEM images of Pt nanoparticles in the Pt/MWNTs after CO annealing are shown in Figure 5c and d, which reveal that the nanoparticle surface is covered largely by the (111) and (100) facets. After analyzing HRTEM images of 22 particles within each sample, the fractions of high-index surface facets of Pt nanoparticles in Pt/MWNTs heat-treated at 573 K were found to decrease after CO annealing, as shown in Figure 1f. Earlier work on single-crystal Pt surfaces[38] has suggested that CO_{ad} can assist the diffusion of Pt adatoms and incorporation into step edges of low-index planes during the CO annealing. Such a process may result in decreased fraction of high-index surface facets on Pt nanoparticles during CO annealing, which presumably diminishes the density of active sites for adsorption of oxygen species and thus reduces CO electro-oxidation activity.

Intrinsic Activity of Pt Nanoparticles for Methanol Electro-oxidation. The specific (Pt-ESA-normalized) activity of methanol electro-oxidation of Pt/MWNT samples was found to increase on Pt nanoparticles obtained from decreasing heat-treatment temperature, as shown in both positive-going and negative-going cyclic voltammetry data in Figure 6a. Cyclic voltammograms of Pt/MWNT samples shown in Figure 6a were recorded typically after 3−5 cycles, and the data no longer changed with subsequent cycling (Figure S9). The cyclic voltammogram data of methanol oxidation on Pt/MWNTs can be explained qualitatively using the following mechanistic understanding established on bulk Pt surfaces. It is well-known that the electrochemical oxidation of methanol follows through two parallel reactions, in which successive dissociative adsorption of methanol to finally form CO_{ad} and oxidation of CO_{ad} on the surface is recognized as the indirect pathway, while methanol oxidation to form soluble intermediates is called the direct pathway.[6,40] Adsorption of methanol first occurs, and continuous dehydrogenation and formation of adsorbed CO is followed as the potential increases.[41] With further increasing potential in the positive-going scan, the dissociation of water begins, which provides the oxygenated species for the Langmuir−Hinshelwood type reaction[6] with adsorbed CO to form CO_2. This reaction rate increases as potential increases until the surface becomes "poisoned" by surface oxygenated species (the coverage of oxygenated species is too high to obtain the maximum reaction rate), which leads to a characteristic oxidation peak in the positive-going scan. At the negative-going scan, oxygenated species are dominant on the surface at the high potential region, and the reaction rate increases with reduction or removal of surface oxygenated species and readsorption of methanol and carbonaceous intermediates with decreasing potential. Eventually, the surface becomes "poisoned" by carbonaceous species such as CO as the potential decreases, which gives rise to a characteristic oxidation peak in the negative-going direction.

Specific currents (based on Pt ESA) at 0.5, 0.6, and 0.7 V vs RHE in the positive-going scan of Pt/MWNT samples were found to increase with decreasing heat-treatment temperature in Figure 6b, indicating higher activity for Pt nanoparticles obtained from lower temperatures (e.g., ∼80 and ∼600 $\mu A/cm^2_{Pt}$ for the 548 K sample vs ∼50 and ∼300 $\mu A/cm^2_{Pt}$ for the 773 K sample at 0.5 and 0.7 V, respectively). Further evidence for enhanced specific activity for methanol electro-oxidation on Pt nanoparticles of lower heat-treatment temperatures is provided in the chronoamperometric measurements. When the potential was stepped from 0.1 to 0.7 V (RHE), the specific current was found to decrease sharply in the first 0.1 s and gradually approach a steady-state value at longer times, as shown in Figure 6c. The Pt/MWNT sample of 573 K, which had a higher fraction of high-index surface facets, was found to have a steady-state specific current after 900 s, which is ∼200% of that of the 773 K sample, as shown in the inset of Figure 6c. It should be noted that the specific current values of Pt/MWNTs after 900 s are comparable to those from cyclic voltammetry data at 0.7 V vs RHE (Figure 6b), which indicates that Pt nanoparticles of ∼2 nm in this study are reasonably stable for methanol oxidation,

(40) Parsons, R.; Vandernoot, T. *J. Electroanal. Chem.* **1988**, *257*, 9–45.
(41) Iwasita, T. *Electrochim. Acta* **2002**, *47*, 3663–3674.

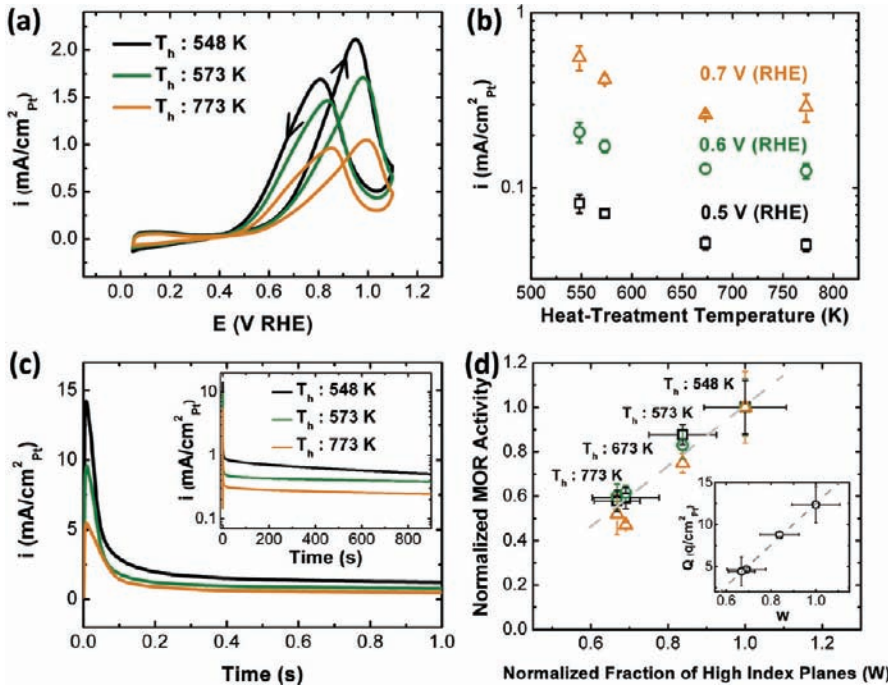

Figure 6. Methanol electro-oxidation activity on Pt/MWNT samples measured at room temperature. (a) Cyclic voltammograms for methanol electro-oxidation of Pt/MWNT samples, where specific current is normalized to the Pt ESA. The data were recorded with 50 mV/s from 0.05 to 1.1 V vs RHE. (b) Specific currents (normalized to Pt ESA) at different potentials (RHE) in cyclic voltammograms. (c) Specific current transients (normalized to Pt ESA) of the electro-oxidation of methanol in the first second, and of the long-time response to 900 s in the inset, which were recorded upon imposing a voltage step from 0.1 to 0.7 V vs RHE. Measurements were conducted in an N_2 saturated solution of 1 M CH_3OH in 0.1 M $HClO_4$. (d) Intrinsic methanol oxidation activity as a function of area fraction of high-index planes normalized to the 548 K sample. Inset compares specific methanol oxidation charge in the positive-going scan of cyclic voltammogram with the area fraction of high-index planes normalized to the 548 K sample. The calculation of error bars can be found in the Experimental Section.

and our cyclic voltammetry data are representative of those under steady-state conditions.

Increasing the electro-oxidation activity of methanol on Pt nanoparticles in the Pt/MWNT samples obtained at lower heat-treatment temperatures in Figure 6a−c can be attributed largely to higher fractions of surface steps shown in Figure 1f. As Pt surface step sites can promote dissociative chemisorption of methanol to form CO_{ad},[7] increased electro-oxidation activity of CO_{ad} observed on Pt nanoparticles obtained from lower temperatures (Figure 3) suggests enhanced reaction kinetics for indirect methanol oxidation. In addition, surface steps on single-crystal surfaces[4] are shown to promote the kinetics of direct methanol oxidation. Therefore, enhanced reaction kinetics for direct methanol oxidation on surface under-coordinated sites of Pt nanoparticles can also contribute to the enhanced intrinsic activity of methanol oxidation on Pt/MWNTs obtained from lower heat-treatment temperatures. To quantify the influence of high-index surface facets of Pt nanoparticles on the intrinsic activity of methanol oxidation, specific current of methanol oxidation in the positive-going cyclic voltammetry scan of Pt/MWNT samples, which was normalized to that of 548 K, is plotted as a function of area fraction of high-index planes normalized to that of 548 K, as shown in Figure 6d. A linear correlation exists between normalized, specific activity for methanol oxidation and normalized area fraction of high-index surface facets for current collected at 0.5, 0.6, and 0.7 V vs RHE. In addition, the specific charge (based on Pt ESA) associated with methanol electro-oxidation in the positive-going scan showed a linear trend with the normalized area fraction of high-index planes, as shown in the inset of Figure 6d.

It should be pointed out that the Pt/MWNT sample of 548 K was found to have considerably higher specific activity (up to an increase of ~200% at 0.5 V vs RHE) for methanol oxidation than did a commercial, supported Pt catalyst (Tanaka Kikinzoku International, Inc.)[42] of a comparable particle size and distribution (Figure 7a). These results show that increasing step densities on Pt nanoparticles of very comparable sizes and size distributions can greatly enhance the intrinsic activity for methanol electro-oxidation, and the magnitude of activity enhancement can be correlated with the amount of surface steps on nanoparticles. In addition, Pt/MWNTs obtained at 573 K showed no loss of activity for methanol electro-oxidation in the potential region from 0.5 to 0.7 V vs RHE during potential cycling from 0.05 to 1.1 V vs RHE in an N_2 saturated solution of 1 M CH_3OH in 0.1 M $HClO_4$ (methanol annealing) up to 250 cycles, as shown in Figure 7b. This result suggests that surface structural changes of Pt nanoparticles associated with methanol electro-oxidation are not significant. It is interesting to contrast that CO annealing leads to significant reduction in the surface step density and activity for CO electro-oxidation, while methanol annealing appears to have no effect on either the surface atomic structure or the activity for methanol electro-oxidation. As previous studies have suggested that CO_{ad} can facilitate surface Pt atom diffusion,[38] greater stability for the methanol electro-oxidation activity on Pt/MWNTs during cycling in a methanol solution than CO electro-oxidation in a CO saturated solution may be attributed to lower surface CO_{ad} on Pt nanoparticles in methanol at high potentials, where further studies are needed to provide details. This finding suggests that Pt nanoparticles

(42) Gasteiger, H. A.; Kocha, S. S.; Sompalli, B.; Wagner, F. T. *Appl. Catal., B* **2005**, *56*, 9–35.

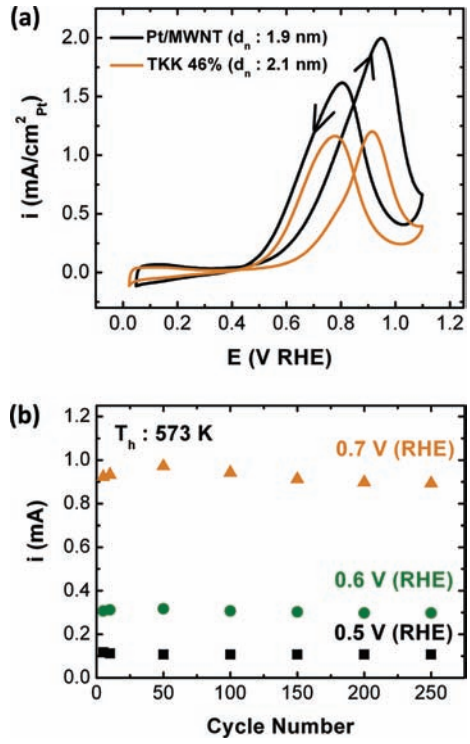

Figure 7. (a) Cyclic voltammograms for methanol electro-oxidation for Pt/MWNTs obtained at 548 K (d_n: 1.9 nm) and a TKK Pt 46 wt % (d_n: 2.1 nm) sample that is commonly used in fuel cells. The potential cycles were recorded at a scan rate of 50 mV/s from 0.05 to 1.1 V (RHE) in a N_2-saturated solution of 1 M CH_3OH in 0.1 M $HClO_4$ at room temperature. (b) Methanol electro-oxidation current of Pt/MWNTs of 573 K as a function of cycle number, which was measured at different potentials (RHE) in the positive-going sweep. The currents were recorded during potential cycling with 50 mV/s from 0.05 to 1.1 V vs RHE in an N_2-saturated solution of 1 M CH_3OH in 0.1 M $HClO_4$ at room temperature.

with increasing surface steps can have long-term activity enhancement and stability for methanol electro-oxidation.

Conclusions

This work, for the first time, characterizes and quantifies the role of surface steps on Pt nanoparticles in electro-oxidation of CO and methanol with sizes of practical relevance. This study demonstrates that insights from single crystal studies are significantly relevant for understanding the behavior of small nanoparticles. A linear relationship between the intrinsic activity (Pt ESA normalized current) and the amounts of surface steps is shown. The CO oxidation activity, together with the incidence of high-index facets on Pt nanoparticles, is reduced after extensive cycling in CO-saturated solution (CO annealing). Interestingly, a corresponding decrease for methanol oxidation activity is not observed upon cycling in methanol. Increasing step densities on Pt nanoparticles of ~2 nm can enhance specific activity based on Pt ESA up to 200% toward electro-oxidation of carbon monoxide and methanol. The enhanced intrinsic activity for methanol electro-oxidation observed in these Pt/MWNT catalysts can translate to reduction of Pt weight up to 200% for a given fuel cell current output. Of significance, this research suggests that strategies to increasing surface steps such as the n(111) × (111) type on nanoparticles offer promise for finding new highly active electrocatalysts for electro-oxidation of small organic molecules.

Experimental Section

High-Resolution Transmission Electron Microscopy. The size and distributions of Pt nanoparticles in Pt/MWNT samples were examined on a JEOL 2010F TEM operated at 200 kV with a point-to-point resolution of 0.19 nm. Pt/MWNT samples were first immersed in Milli-Q 18 MΩ water and subsequently dispersed ultrasonically for 5 min. The suspension was then deposited on a lacey carbon grid and dried in air for TEM observations. At least 200 randomly selected nanoparticles from HRTEM images were used to produce each particle size distribution. For each distribution, the number-averaged diameter, d_n, was determined by $d_n = (\Sigma_{i=1}^{n} d_i)/n$. The error bars of d_n in Figure 1b are defined as the standard deviations of the mean (SDOM), $\sigma_x/\sqrt{N}$, where σ_x is the standard deviation of d_n in each sample, and N is the number of particles in each histogram.

The indexes of surface facets of Pt nanoparticles were determined from the HRTEM images. The FFT of a HRTEM image was performed with Digital Micrograph (Version 3.11.2, Gatan Inc., Pleasanton, CA). With the aid of Digital Micrograph, the interplanar distance and the angle between atomic planes were obtained from FFT images, which allowed indexing of lattice fringes and surface facets in the HRTEM images. The average fraction of high-index planes in each Pt/MWNT sample as a function of heat-treatment temperature was obtained by summing the product of average fraction of high-index surface within each bin (right axis) and the frequency (left axis) of the bin in the histogram of Figure S2a−d. The error bars in Figure 5a,b and Figure S2a−d, σ_i, are defined as the standard deviations of the mean (SDOM), $\sigma_0/\sqrt{N}$, where σ_0 is the standard deviation of the fraction of high-index planes in each bin, and N is the number of particles in the bin. The error bars in Figure 1f are equal to $[\Sigma(\sigma_i f_i)^2]^{1/2}$, where f_i is the frequency (left axis) for each bin in Figure S2a−d, and σ_i is the SDOM of the high-index plane fraction determined in the same bin. The fraction of high-index surface facets was obtained from analyzing at least 14 particles for each sample (Figures S2 and 5).

Ultraviolet Photoelectron Spectroscopy. Pt/MWNT and MWNT [functionalized MWNT-COOH by acid treatments from ref 20 and references therein, which was then heat-treated at 300 °C in H_2 for 2 h] powder was deposited on clean highly ordered pyrolytic graphite (SPI Supplies). UPS measurements were performed at the U5UA beamline at the National Synchrotron Light Source at the Brookhaven National Laboratory. The ultraviolet photoemission spectra were collected with a 125 mm hemispherical analyzer at photon energies of 80 and 130 eV under ultra high vacuum conditions of 5×10^{-11} Torr. The total instrument resolution was set to 0.10 eV. As the photoemission cross section of Pt is dominated by the d states at 80 eV because the cross section of s and p states is much smaller than that of the d states, the valence band structure measured mostly reflects the valence d states.[30] To obtain the photoemission contribution from Pt nanoparticles only, the density of states of MWNT was subtracted from those of Pt/MWNT samples. This method has been previously used by Eberhardt et al.[29] The d band center energy relative to the Fermi level was calculated from $d_\varepsilon = \int N(\varepsilon)\varepsilon\, d\varepsilon / \int N(\varepsilon)\, d\varepsilon$, where $N(\varepsilon)$ is the density of states.[31]

Electrode Preparation. Pt/MWNT powder was well dispersed in Milli-Q 18 MΩ water using an ultrasonicator (Sonics & Materials, Inc.). Twenty microliters of suspension was dropped on the glassy carbon electrode (5 mm in diameter), resulting in Pt loading in the range of 10−30 $\mu g/cm^2_{electrode}$. Uniform, thin Pt/MWNT films were prepared by evaporation of the water, and followed by dropping 10 μL of a dilute Nafion solution (0.025 wt %), which was prepared from 5 wt % Nafion solution (Ion Power, Inc.). Only freshly prepared Pt/MWNT electrodes were used to measure electrochemical activity. A commercial Pt nanoscale catalyst sample supported on high surface area carbon [Tanaka Kikinzoku International, Inc.] with a metal loading of 46 wt %, which is commonly used in fuel cells,[42] was used for comparison.

Electrochemical Measurements. All electrochemical measurements were performed in a three-electrode cell at room temperature. A Pt wire and a saturated calomel electrode (SCE) (Analytical Sensor, Inc.) were used as the counter and reference electrodes,

respectively. SCE potential was calibrated to the RHE scale. Cyclic voltammetry measurements were performed in O_2-free 0.1 M $HClO_4$ electrolyte obtained by bubbling ultra high-purity N_2 gas (99.999%, Airgas) for at least 30 min. The electrodes were cycled with the potential range between 0.05 and 1.1 V (RHE) to reach steady-state cyclic voltammograms at a scan rate of 20 mV/s. Pt ESA was determined from the charge associated with hydrogen adsorption (210 $\mu C/cm^2_{Pt}$) after double layer correction in the cyclic voltammetry data between 0.05 and 0.35 V vs RHE. For CO stripping and CO chronoamperometric measurements, activity was measured in 0.1 M $HClO_4$ CO-free electrolyte with a scanning rate of 5 mV/s, which was obtained by bubbling ultra high-purity N_2 gas (99.999%, Airgas) for at least 30 min, after complete adsorption of CO at a potential of 0.1 V (RHE). To prevent irreversible changes of Pt surface structure in CO atmosphere (typically referred to as CO annealing),[18] no electrochemical cycling of electrode in CO-saturated electrolyte was performed before any electrochemical measurements. To evaluate the activity of bulk CO electro-oxidation, current was obtained from scanning a RDE in a CO-saturated solution as a function of potential vs RHE (Figure S8). Current in the first cycle was recorded at 1600 rpm, which was used to calculate the specific activity in the inset of Figure 3c to minimize the effect of CO annealing on the surface atomic structure of Pt nanoparticles. CO-annealed Pt/MWNT samples were obtained after cycling in a CO-saturated 0.1 M $HClO_4$ solution from 0.1 to 1.1 V vs RHE at a scan rate of 50 mV/s for 10 min. The activity of methanol electro-oxidation was evaluated by cyclic voltammetry in an N_2-saturated solution of 1 M CH_3OH in 0.1 M $HClO_4$ with a scanning rate of 50 mV/s. At least four experimental data sets were collected to generate the error bars in Figure 6b and d, which were defined as the standard deviations of specific current (normalized to Pt ESA). The charge associated with methanol oxidation in the positive-going scan of cyclic voltammogram data was calculated by the integration of the positive-going current between ~0.35 and 1.1 V vs RHE after subtraction of the double layer current, which was used to generate the inset of Figure 6d. Methanol electro-oxidation stability of Pt/MWNT samples was measured during cycles with 50 mV/s from 0.05 to 1.1 V vs RHE in an N_2-saturated solution of 1 M CH_3OH in 0.1 M $HClO_4$ at room temperature.

Acknowledgment. This work was supported in part by the DOE Hydrogen Initiative program under award number DE-FG02-05ER15728 and Toyota Motor Co. This work made use of the Shared Experimental Facilities supported by the MRSEC Program of the National Science Foundation under award number DMR 02-13282. S.W.L. acknowledges a Samsung Scholarship, Samsung Foundation of Culture. The National Synchrotron Light Source, Brookhaven National Laboratory, is supported by the U.S. Department of Energy, Office of Science, Office of Basic Energy Sciences. We would like to thank N. Marzari and H. A. Gasteiger at MIT for fruitful discussions.

Supporting Information Available: Representative HRTEM micrographs of Pt/MWNT samples, particle size histograms and fraction of high-index surfaces projected on the particle perimeter along the [110] zone axis as a function of d_n for Pt/MWNT samples, schematics showing the area fraction of (100) and (111) planes on an ideal truncated octahedron crystal and the length fraction of the corresponding planes on the crystal perimeter along the [110] zone axis, Pt core level ($4f_{7/2}$) shifts of Pt/MWNTs obtained at different temperatures relative to bulk Pt, an example of k^3-weighted Fourier transform for Pt/MWNT samples from the analysis of extended X-ray absorption fine structure (EXAFS) at the Pt L_3-edge, changes in the coordination numbers (CN) of Pt−O and Pt−Pt nearest neighbors and the change in d band vacancy relative to Pt foil as a function of heat-treatment temperature, CO stripping voltammetry and current transients of the oxidation of CO adlayer of Pt/MWNTs, CO bulk oxidation of Pt/MWNTs obtained at 773 K using a rotation disk electrode, and cyclic voltammograms for methanol oxidation reaction for Pt/MWNTs obtained at 573 K. This material is available free of charge via the Internet at http://pubs.acs.org.

JA9025648